



Universiteit
Leiden
The Netherlands

Asp179 in the class A β -lactamase from *Mycobacterium tuberculosis* is a conserved yet not essential residue due to epistasis

Alen, I. van; Chikunova, A.; Zanten, D.B. van; Block, A.A. de; Timmer, M.; Brünle, S.; Ubbink, M.


Citation

Alen, I. van, Chikunova, A., Zanten, D. B. van, Block, A. A. de, Timmer, M., Brünle, S., & Ubbink, M. (2023). Asp179 in the class A β -lactamase from *Mycobacterium tuberculosis* is a conserved yet not essential residue due to epistasis. *Febs Journal*, 290, 4933-4949. doi:10.1111/febs.16892

Version: Publisher's Version
License: [Creative Commons CC BY 4.0 license](https://creativecommons.org/licenses/by/4.0/)
Downloaded from: <https://hdl.handle.net/1887/3656947>

Note: To cite this publication please use the final published version (if applicable).

Asp179 in the class A β -lactamase from *Mycobacterium tuberculosis* is a conserved yet not essential residue due to epistasis

Ilona van Alen, Aleksandra Chikunova, Danny B. van Zanten, Amber A. de Block, Monika Timmer, Steffen Brünle and Marcellus Ubbink 

Leiden Institute of Chemistry, Leiden University, Leiden, The Netherlands

Keywords

crystal structure; enzyme; protein evolution; β -lactamase

Correspondence

M. Ubbink, Leiden Institute of Chemistry, Leiden University, Einsteinweg 55, 2333 CC Leiden, The Netherlands.
 Tel.: +31 71 5274628
 E-mail: m.ubbink@chem.leidenuniv.nl

Ilona van Alen and Aleksandra Chikunova contributed equally to this work.

(Received 30 January 2023, revised 22 May 2023, accepted 15 June 2023)

doi:10.1111/febs.16892

Conserved residues are often considered essential for function, and substitutions in such residues are expected to have a negative influence on the properties of a protein. However, mutations in a few highly conserved residues of the β -lactamase from *Mycobacterium tuberculosis*, BlaC, were shown to have no or only limited negative effect on the enzyme. One such mutant, D179N, even conveyed increased ceftazidime resistance upon bacterial cells, while displaying good activity against penicillins. The crystal structures of BlaC D179N in resting state and in complex with sulbactam reveal subtle structural changes in the Ω -loop as compared to the structure of wild-type BlaC. Introducing this mutation in four other β -lactamases, CTX-M-14, KPC-2, NMC-A and TEM-1, resulted in decreased antibiotic resistance for penicillins and meropenem. The results demonstrate that the Asp in position 179 is generally essential for class A β -lactamases but not for BlaC, which can be explained by the importance of the interaction with the side chain of Arg164 that is absent in BlaC. It is concluded that Asp179 though conserved is not essential in BlaC, as a consequence of epistasis.

Introduction

In protein families sets of highly conserved amino acid residues can be identified. Conservation is used as a proxy for essentiality because mutations in these residues are evidently not tolerated due to loss of function. The equation of conservation and essentiality is valid as an argument to explain conservation, but it does not mean that a conserved residue is essential in every member of the protein family. Epistatic effects influence the role of residues and the essential nature of the residue may be lost without the residue being mutated. An example of such a case is described here. In a recent study from our laboratory all the second and third-shell conserved

residues in the class A β -lactamase BlaC from *Mycobacterium tuberculosis* were mutated [1]. In line with expectation, mutation of most conserved residues resulted in non-functional enzyme. The distance from the active site was correlated with the function of the residues. Third-shell conserved residues, far from the active site, were shown to be essential for solubility and folding. Second-shell residues, around the active site, contribute to stabilizing the single catalytically most active conformation [1]. Interestingly, this broad mutagenesis study also revealed that for some conserved residues certain mutations functioned equally or better than the wild-type enzyme in

Abbreviations

CD, circular dichroism; CSP, chemical shift perturbation; IPTG, Isopropyl β -D-1-thiogalactopyranoside; NMR, nuclear magnetic resonance; RMSD, root-mean-square deviation; SDS-PAGE, sodium dodecyl sulphate–polyacrylamide gel electrophoresis; TAT, twin-arginine translocation; TEV, Tobacco Etch Virus.

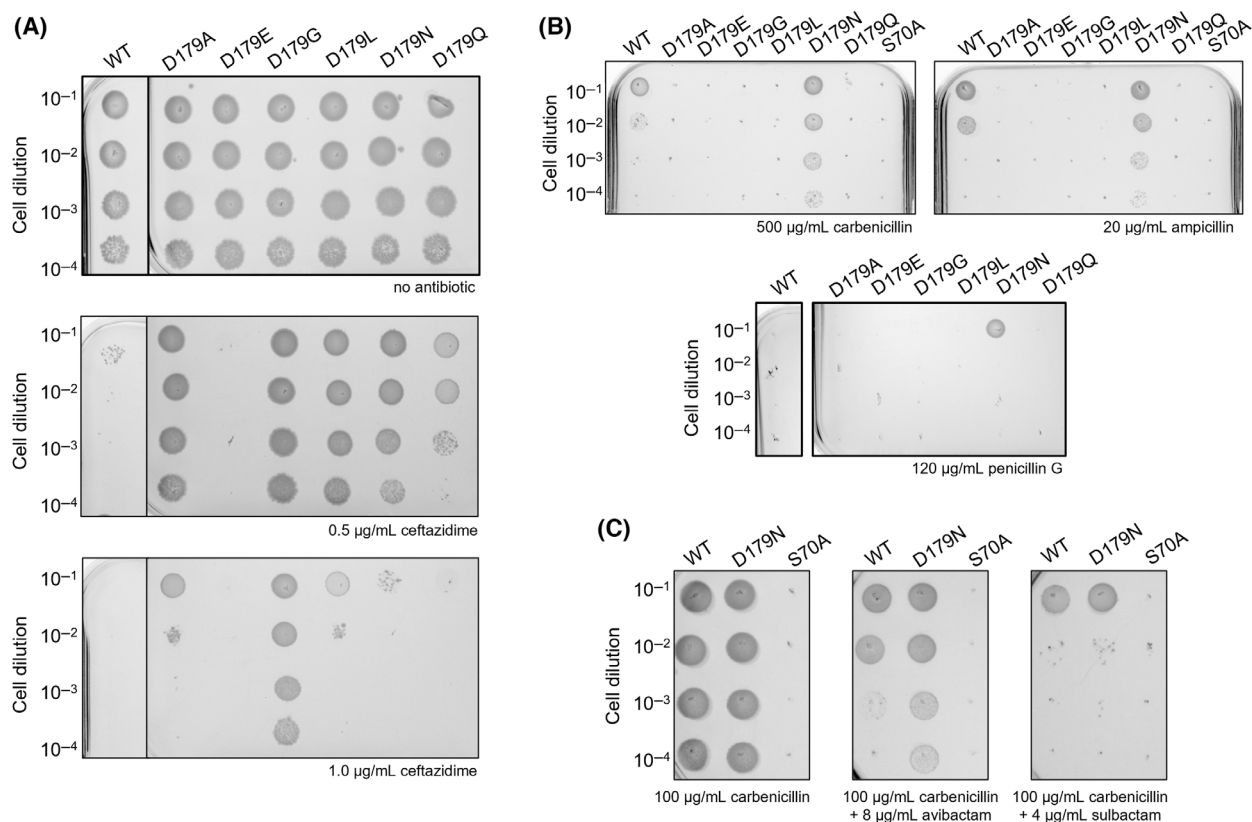


Fig. 1. Cell growth assays. Drops of increasing dilutions of *E. coli* cultures were spotted on LB-agar plates containing the indicated antibiotics and inhibitors, as well as kanamycin (50 $\mu\text{g}/\text{mL}$) to ensure plasmid stability and 1 mM IPTG to induce gene expression. The plates were incubated at 37 $^{\circ}\text{C}$ for 16 h. (A) Ceftazidime. Wild-type BlaC panels are from the same LB-agar plates as BlaC variants (Fig. S1 shows complete photos); (B) Carbenicillin, ampicillin, and penicillin G (Figs S1 and S2 show complete data set). (C) Inhibitors sulbactam and avibactam in the presence of 100 $\mu\text{g}/\text{mL}$ carbenicillin. BlaC S70A is catalytically inactive and functions as negative control.

activity against ampicillin, raising the question whether these conserved residues were essential.

Here, we focus on residue Asp179 (Ambler numbering [2]), which is present in 99.8% of the enzymes in this family [1]. Asp179 is located in the Ω -loop of the protein, a loop that also contains Glu166, the general acid/base involved in deacylation of the enzyme, which is the second step in the catalytic mechanism [3–5]. In BlaC, the mutation D179N led to an increase in resistance against penicillins of *Escherichia coli* cells, together with slightly increased thermostability of the purified enzyme [1]. However, substitution of any other residue for Asp179 in TEM-1 and KPC-2 has been reported to result in less fitness, except when using ceftazidime as a substrate [6–11]. These results lead to the hypothesis that Asp179 is essential in other β -lactamases but not in BlaC, despite being conserved. To test this idea, BlaC D179N was characterized in more detail and its fitness was compared with the same variant constructed in several other β -lactamases, representative of the class A β -lactamase family. Our

results show that the mutation D179N indeed decreases general fitness of other β -lactamases, contrary to BlaC. The crystal structure of BlaC D179N offers an explanation for the loss of the essentiality of Asp179.

Results

BlaC D179 variants show different substrate specificity

To investigate the importance of the side chain in position 179 of BlaC, the Asp was mutated to Ala, Glu, Gly, Leu, Asn, and Gln. *E. coli* cultures producing Asp179 variants in the periplasm were tested for resistance against various antibiotic compounds. The minimum concentration at which the cells could not grow was determined by applying drops of cell culture of OD_{600} 0.3–0.0003 on agar plates, containing the penicillins ampicillin, carbenicillin or penicillin G, or the third-generation cephalosporin ceftazidime (Fig. 1,

Table 1. Concentrations of various β -lactams and β -lactamase inhibitors at which growth of *E. coli* producing BlaC variants is no longer observed, determined with the droplet test (Fig. 1, Figs S1 and S2). All values are in $\mu\text{g mL}^{-1}$. Catalytically inactive BlaC S70A was used as a negative control.

BlaC variant	Ampicillin	Ceftazidime	Carbenicillin	Penicillin G	Avibactam ^a	Sulbactam ^a
Wild-type	120	0.8	>1000	120	>16	5
S70A	3	0.2	20	40	ND	ND
D179A	10	2	100	80	ND	ND
D179E	3	0.2	20	40	ND	ND
D179G	5	5	100	40	ND	ND
D179L	3	2	20	40	ND	ND
D179N	120	2	>1000	>120	>16	7.5
D179Q	5	1	20	40	ND	ND

^aInhibitors were used in combination with $100 \mu\text{g mL}^{-1}$ carbenicillin. ND, not determined.

Figs S1 and S2). In our experience, this approach allows for subtler differences in antibiotic resistance to be detected than standard MIC determination. For the evaluation of β -lactamase inhibitor susceptibility, $100 \mu\text{g mL}^{-1}$ carbenicillin was used in combination with the β -lactam inhibitor sulbactam and non- β -lactam inhibitor avibactam. The results indicate that almost all tested Asp179 mutants outperformed wild-type against ceftazidime. This antibiotic is a poor substrate for BlaC. In the used assay, cells producing wild-type BlaC do not grow on plates with $0.8 \mu\text{g mL}^{-1}$ ceftazidime, compared with $0.2 \mu\text{g mL}^{-1}$ for the negative control, BlaC S70A. For comparison, for ampicillin and carbenicillin, cells stop growing at $120 \mu\text{g mL}^{-1}$ and $>1000 \mu\text{g mL}^{-1}$, respectively (Table 1). Of the D179 variants, BlaC D179G shows the largest increase, a more than six-fold increase in the minimum concentration that inhibited growth (Fig. 1A, Table 1). However, only cells producing BlaC D179N displayed increased growth in presence of other β -lactam antibiotics (Fig. 1B, Figs S1 and S2, Table 1) and they also showed somewhat higher resistance to avibactam, which probably can be attributed to an increased conversion of carbenicillin that was used in combination with inhibitors (Fig. 1C). It is concluded that mutation of Asp179 in BlaC shifts the substrate specificity from penicillins to ceftazidime, except for BlaC D179N, which outperforms wild-type BlaC on both types of substrates.

BlaC D179N has a higher melting temperature than wild-type

To characterize the BlaC variants further, the enzymes were overproduced in the cytoplasm of *E. coli*. The yield of soluble BlaC D179E from 1 L of cell culture was lower than for the other BlaC variants and most protein was insoluble (Fig. 2A). Other BlaC variants

were produced in quantities similar to BlaC wild-type, except for BlaC D179N, for which production was slightly increased. All mutants, except for D179E, exhibited the same secondary structure content as wild-type BlaC, as judged by CD spectroscopy (Fig. 2B). Denaturation experiments were performed to establish the thermal stability of the BlaC variants. Both tryptophan fluorescence and a thermal shift assay with hydrophobic dye were used for melting temperature assessment, as these methods might yield structure specific results. Substitution of Asp179 with Asn resulted in 1.5°C increase in melting temperature, whereas substitutions to Gly, Gln and Ala significantly lowered melting temperature (Table 2, Fig. 2B). For BlaC D179E and D179L the unfolding curves did not show a clear melting point.

BlaC D179G and D179N exhibit different kinetic profiles

The kinetic parameters of nitrocefin hydrolysis of BlaC D179N, BlaC D179G and WT BlaC were measured using purified enzymes. BlaC D179N displayed a nitrocefin activity very similar to that of the wild-type BlaC with catalytic efficiencies of $4.0 \pm 0.3 \times 10^5 \text{ M}^{-1} \text{ s}^{-1}$ and $3.3 \pm 0.3 \times 10^5 \text{ M}^{-1} \text{ s}^{-1}$ for wild-type BlaC and BlaC D179N respectively (Table 3, Fig. 3A). An *in vitro* inhibition assay with avibactam indicated no reduced sensitivity of this mutant for the inhibitor (Fig. 3B). Therefore, we attribute the slightly higher resistance of cells producing BlaC D179N as compared to wild-type BlaC to an elevated level of active enzyme, and the increased resistance of the cells to avibactam to concomitant faster degradation of the antibiotic. The overexpression results (Fig. 2A) and somewhat higher melting temperature suggest a higher stability of the soluble enzyme, and, thus, the level of active BlaC D179N in the cell assay may well be

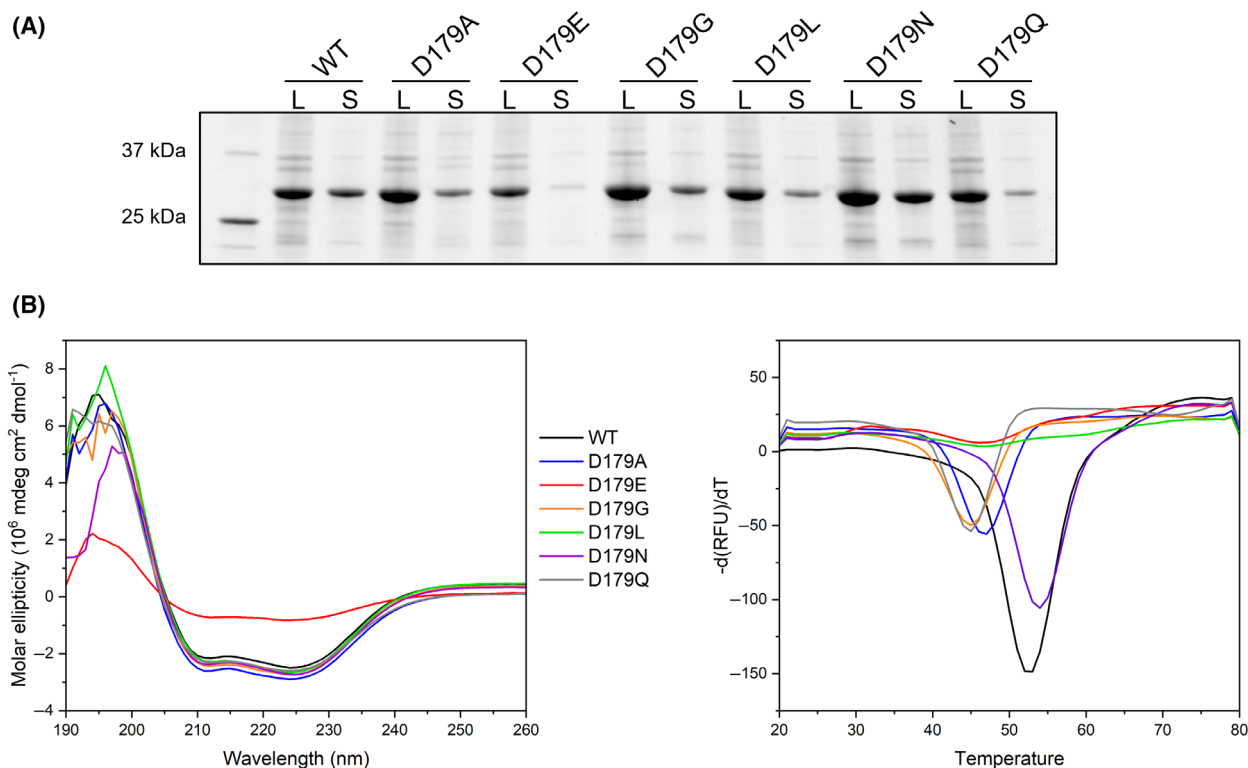


Fig. 2. Production, folding and stability of BlaC variants. (A) SDS-PAGE analysis shows the whole lysate (L) and soluble fraction (S) after production of wild-type BlaC and BlaC D179 mutants using a cytoplasmic overexpression system. (B, left) CD spectra of BlaC Asp179 mutants. (B, right) Negative derivative of signal from thermal shift assay with the hydrophobic dye SYPRO® Orange of BlaC Asp179 mutants. The melting temperatures are listed in Table 2.

Table 2. Melting temperatures for BlaC variants. SD represents the standard deviation of three measurements. The two methods do not necessarily report the same conformational change making the melting temperature method-dependent.

	Tryptophan fluorescence		Hydrophobic dye	
	$T_m \pm SD$ (°C)	$\Delta T_m \pm SD$ (°C)	T_m (°C)	ΔT_m^a (°C)
Wild-type	62.0 ± 0.1	0	52.0 ± 0.5	0
D179A	54.8 ± 0.2	-7.2 ± 0.2	47.0 ± 0.5	-5
D179G	51.4 ± 0.2	-10.6 ± 0.2	45.0 ± 0.5	-7
D179N	63.3 ± 0.1	1.3 ± 0.1	53.5 ± 0.5	1.5
D179Q	50.70 ± 0.05	-11.3 ± 0.1	45.0 ± 0.5	-7

^aError 0.7 °C.

higher than that of wild-type enzyme. Purified BlaC D179G does not display any activity against nitrocefin (Fig. 3C). However, activity against the poor substrate ceftazidime benefits from both the Asp-to-Asn and Asp-to-Gly substitution (Table 3), with 2.5- and >20-fold increase of k_{cat}/K_M parameters, respectively, in line with the findings of the cellular assay. Ceftazidime degradation with BlaC D179G clearly displays two

phases (Fig. 3D), so the standard steady-state model is not applicable. At lower enzyme concentration, two phases can be distinguished also for wild-type BlaC and BlaC D179N (Fig. 3E). We used the second linear phase to calculate the velocity of the reaction. Two-phase ceftazidime hydrolysis was observed and explained before for KPC-2 β -lactamase with the burst phase caused by rapid acylation and the following linear phase by slow deacylation [12]. This explanation does not apply to BlaC, as the amplitude of the burst phase indicates that the enzyme molecules perform more than a single turnover and the amount of product formed in the first phase is dependent on the substrate concentration. The substrate dependence of the second phase of BlaC D179G indicates a low apparent K_M (Table 3, Fig. 3F), suggesting a rate constant of acylation that is much larger than of deacylation. For wild-type and D179N BlaC, the apparent K_M is high and only the k_{cat}/K_M can be determined (Fig. 3F). It is probable that BlaC D179G (and to small extent also wild-type and D179N BlaC) exists in two conformations that react differently with ceftazidime. Such two-phase kinetics for ceftazidime has previously been

Table 3. Apparent Michaelis–Menten kinetic parameters for nitrocefin and ceftazidime hydrolysis. Reactions were carried out in 100 mM sodium phosphate buffer (pH 6.4) at 25 °C. Standard deviations (SD) are calculated from triplicate measurements for nitrocefin and duplicate measurements for ceftazidime. ND, not determined.

BlaC variant	Nitrocefin			Ceftazidime		
	$K_M \pm \text{SD}$ (μM)	$k_{\text{cat}} \pm \text{SD}$ (s^{-1})	$k_{\text{cat}}/K_M \pm \text{SD}$ ($10^5 \text{M}^{-1} \text{s}^{-1}$)	K_M (μM)	$k_{\text{cat}} \pm \text{SD}$ (s^{-1})	$k_{\text{cat}}/K_M \pm \text{SD}$ ($10^3 \text{M}^{-1} \text{s}^{-1}$)
Wild-type	263 \pm 17	106 \pm 5	4.0 \pm 0.3	ND	ND	0.09 \pm 0.01
D179N	297 \pm 24	98 \pm 6	3.3 \pm 0.3	ND	ND	0.24 \pm 0.02
D179G	ND	ND	ND	<5	(1.0 \pm 0.2) $\times 10^{-2}$	>2

published for TEM-1 W165Y/E166Y/P167G and PenI C69F and suggests a branched pathway for substrate hydrolysis [13,14]. Such kinetics have also been observed for other BlaC variants [15] and will be described in more detail elsewhere.

BlaC D179N shows subtle conformational changes in comparison to wild-type BlaC

Structural characterization focused on BlaC D179N. NMR spectroscopy of BlaC D179N confirmed that this variant is well-folded (Fig. S3). ^1H and ^{15}N chemical shifts of backbone amide resonances of the mutant protein were assigned and compared to those of wild-type BlaC (Fig. 4). The largest chemical shift perturbations (CSPs) due to the mutation are observed for amides in the Ω -loop but smaller CSPs spread out over other parts of the structure. The crystal structure of the BlaC D179N solved at 1.8 Å resolution reveals the nature of the structural changes (Table S1, Figs 5 and 6). Overall, the structure of the mutant resembles the BlaC wild-type structure ($C\alpha$ RMSD 0.31 Å, Fig. 5). Surprisingly, the newly introduced asparagine occupies the same location as the side chain of aspartate (Fig. 5B) and the interactions of D179 are conserved. In the structure of wild-type BlaC, the carboxy-carboxylate interaction requires a shared proton between Asp172 and Asp179 [16,17], in BlaC D179N this interaction likely is an ordinary hydrogen bond between γ -carboxy group of Asp172 and NH_2 of the amide group of Asn179. Despite the conserved interactions, some changes are observed in the Ω -loop of the mutant. Two peptide bonds, involving Pro174-Gly175 and Arg178-Asn179 are flipped in BlaC D179N (Fig. 6A,B). The flipped bond involving Arg178 is accompanied by the loss of salt bridges between Arg178 and Asp172 and Asp163 and Arg161. Asp163 was found in two conformations, one of which is rotated toward the solvent and the created space is occupied by the backbone carbonyl of Arg178. The second conformation is still able to form a salt bridge

with Arg161, but both Asp163 and Arg161 are pushed away from the loop containing Arg178. Previously, our group solved the structures of wild-type BlaC with the inhibitors clavulanic acid, sulbactam, tazobactam, and avibactam, as well as BlaC G132S with sulbactam [18,19]. Here, we solved the structures of BlaC D179N with inhibitors sulbactam and vaborbactam at 1.9 Å, as well as structure of BlaC wild-type with vaborbactam (Fig. 5C,D) as no structures of BlaC with this transition state inhibitor were available. Both inhibitors occupied the binding pocket of the BlaC D179N in the same way as in the wild-type enzyme (Fig. 5E, F). In the structure of BlaC D179N with sulbactam, however, only the Pro174-Gly175 peptide bond was found flipped, while in the structure of BlaC D179N with vaborbactam both Pro174-Gly175 and Arg178-Asn179 were found in the same conformation as in the wild-type BlaC (Fig. 6C). These observations suggest an increased conformational freedom of this region of the Ω -loop in BlaC D179N, compared to the wild-type enzyme. However, the NMR spectra did not provide evidence for millisecond dynamics (no line broadening) and normalized B-factor analysis did not show any significant difference between the Ω -loop in the wild-type structures and the D179N variant structures (Fig. 6E). Combined, these findings do not suggest that BlaC D179N has strongly increased dynamics in the Ω -loop. The comparison of the B-factors shows a few differences in the solvent exposed loops distant from the mutation site that might be explained by the crystal packing or pH differences in the crystallization. The structure of wild-type BlaC bound to trans-enamine adduct of sulbactam displays increased normalized B-factors of the residues 99–107 located in the loop on top of the binding pocket, compared to those of the BlaC D179N sulbactam adduct, which might indicate the importance of the Asp179 residue for the selectivity of the substrate binding, as the residues within this loop were shown to be involved in substrate recognition, or be the result of a slightly different position of the adduct in the active site (Fig. 5E).

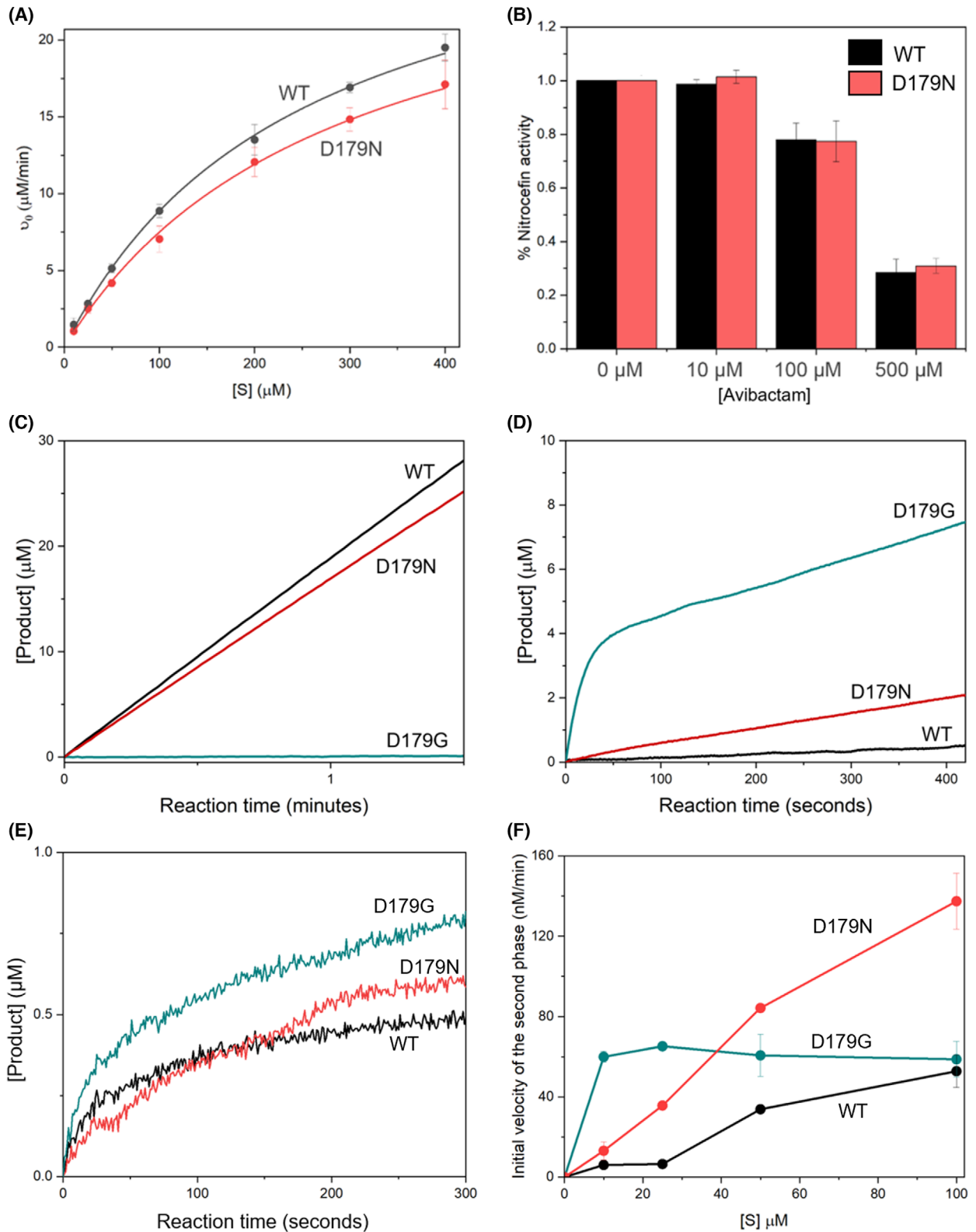


Fig. 3. Kinetic analysis (A) Michaelis–Menten curves for reaction with nitrocefim of BlaC wild-type and D179N. Error bars represent standard deviations of triplicates and curves represent the fit to the Michaelis–Menten equation (eq. 1); (B) Relative activity in the absence or presence of avibactam and BlaC measured as amount of hydrolyzed nitrocefim after 20 min at 25 °C. Measurements were performed in duplicate in the presence of 100 μ M nitrocefim and 2.5 nM BlaC. The error bars represent one standard deviation. (C) Product formation curves with 400 μ M nitrocefim and 5 nM BlaC as a function of time; (D) Product formation curves with 20 μ M ceftazidime and 1 μ M BlaC. (E) Product formation curves with 50 μ M ceftazidime and 100 nM BlaC as a function of time. Data were obtained in 100 mM sodium phosphate buffer (pH 6.4) at 25 °C by measuring a change in absorbance at 486 and 260 nm for nitrocefim and ceftazidime, respectively; (F) The initial velocities of the second phase of the ceftazidime degradation reaction as a function of initial ceftazidime concentration. Error bars represent standard deviations of duplicate experiments.

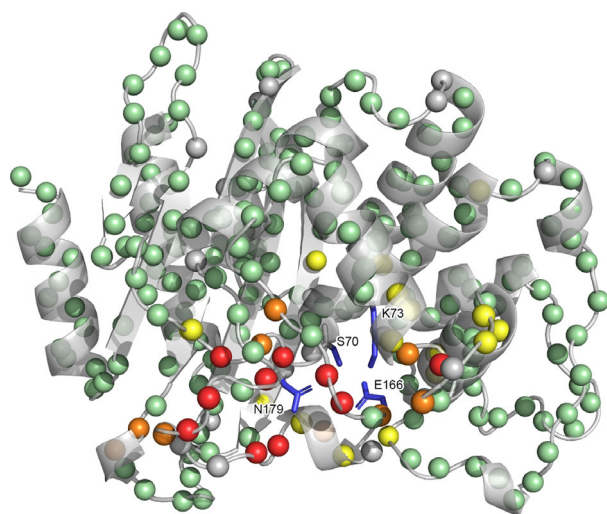


Fig. 4. Average chemical shift differences (CSP) between the amide resonances of BlaC D179N and wild-type BlaC mapped on the structure of BlaC D179N (PDB entry 8BTU). Residues are coloured green for CSP < 0.025, yellow for CSP > 0.025 ppm, orange for CSP > 0.05 ppm, red for CSP > 0.1 ppm and grey for no data, backbone amide nitrogen atoms are represented as spheres. Side chains of active site residues and N179 are represented as blue sticks, the entrance to the active site is at the back of the protein in this representation. The figure is generated using The PyMOL Molecular Graphics System, Version 2.5.0 (Schrödinger, LLC, New York, NY, USA).

The D179N mutation is detrimental in other class A β -lactamases

To investigate why residue 179 does not appear as an asparagine in class A β -lactamases, the D179N mutation was introduced in four BlaC orthologues. These β -lactamases were selected based on sequence identity (Table 4, Fig. 7), structural root-mean-square deviation (RMSD), and available information from previous research. CTX-M-14, KPC-2, NMC-A, and TEM-1 share on average 42% of their sequences with BlaC, which is less than the average sequence identity of 50% found for 497 class A β -lactamase sequences. The average RMSD for the C α atoms of CTX-M-14, KPC-2, NMC-A, and TEM-1 compared to BlaC is 0.79 Å (Table 4). The genes coding for the soluble

parts of these β -lactamases and their D179N variants were cloned in the same expression vector as *blaC*, behind a signal peptide for TAT-based translocation [19]. The ability to convey resistance to *E. coli* against antibiotics was tested as described for the BlaC variants. For both ampicillin and meropenem, the cells expressing the wild-type variants of CTX-M-14, KPC-2, NMC-A and TEM-1 grow better than the cells expressing D179N variants, whereas this is not the case for BlaC (Fig. 8, Figs S4–S7). This trend was also observed for carbenicillin, although NMC-A did not confer any resistance at the concentrations used for this assay (Fig. 8, Fig. S5). Interestingly, cells expressing the D179N variants for carbapenemases NMC-A and KPC-2 grow better on ceftazidime than cells expressing the wild-type variant, whereas cells expressing TEM-1 did not grow at all on the concentrations tested. These differences in growth were also observed when growing the cells in liquid cultures (Figs S8–S11). Cells producing TEM-1 grow worse in the presence of ampicillin than ones making BlaC, which is surprising because TEM-1 is known to be quite active against ampicillin. Perhaps the expression system used in this study is less suitable for TEM-1 than for BlaC. So, in summary, and contrary to what was observed for BlaC, the D179N mutation negatively affects the ability of *E. coli* cells to grow in presence of penicillins or meropenem for all four β -lactamases, CTX-M-14, KPC-2, NMC-A and TEM-1, either because the mutation changes the catalytic properties or leads to reduced levels of active enzyme.

The *in vitro* activity of the β -lactamases was tested using the soluble cell fractions and nitrocefim as substrate, following an approach described before [1]. For these experiments, the genes were cloned in overexpression vectors with T7 promoter and cytoplasmic expression, as used for the BlaC production. Wild-type BlaC and BlaC D179N exhibit comparable protein levels and nitrocefim activity. However, large differences were observed for the other β -lactamases (Fig. 9). Wild-type CTX-M-14 and TEM-1 were better at nitrocefim hydrolysis than BlaC while their D179N variants were insoluble and no activity could be detected in the

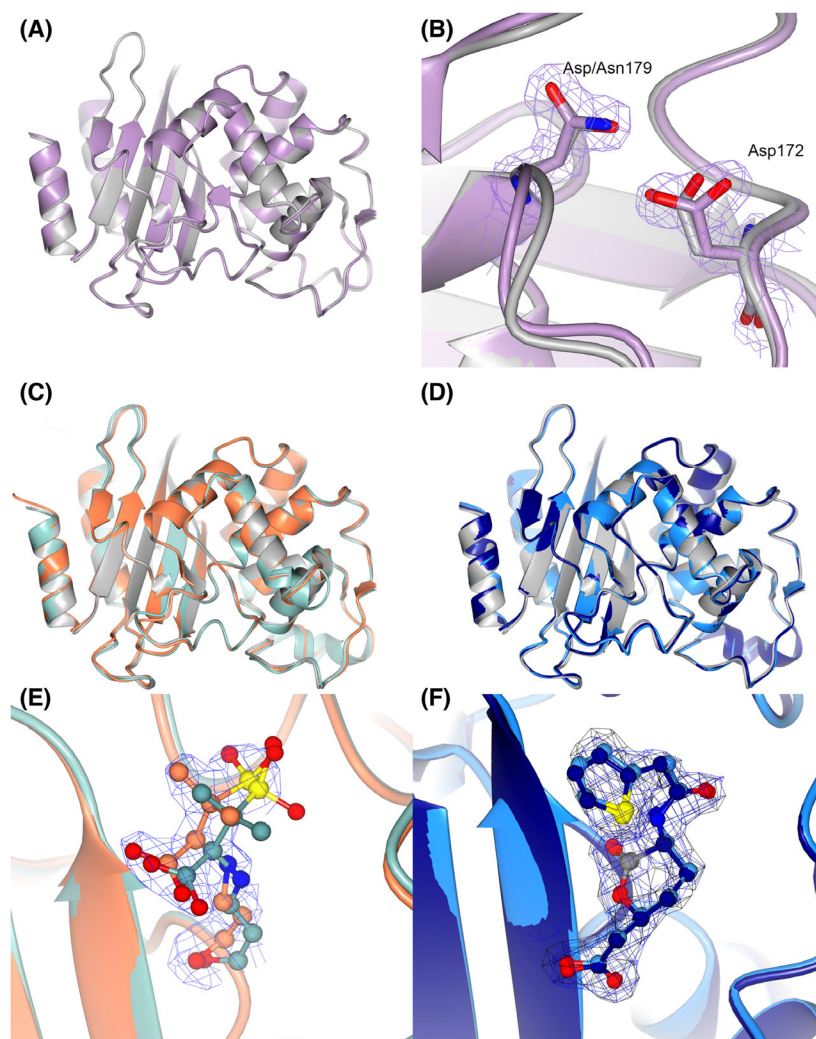


Fig. 5. (A) Crystal structure of BlaC D179N (PDB entry [8BTU](#), lilac) overlaid with wild-type structure (PDB entry [2GDN](#) [3], grey); (B) Detail of the region around the mutation. The 2mF0-DFc electron density map for BlaC D179N is centered on labelled residues and is shown in purple chicken wire, with contour level 1σ and extent radius 5 \AA ; (C) Crystal structure of BlaC D179N with sulbactam (PDB entry [8BTU](#), orange) overlaid with wild-type structure free form (grey) and with sulbactam (PDB entry [6H2K](#) [18], turquoise); (D) Crystal structure of BlaC D179N with vaborbactam (PDB entry [8BTW](#), light blue) overlaid with wild-type structure, free form (grey) and with vaborbactam (PDB entry [8BV4](#), dark blue); (E,F) position of inhibitors sulbactam (E) and vaborbactam (F), respectively in BlaC wild-type (turquoise and dark blue, respectively) and BlaC D179N (orange and light blue, respectively). The 2mF0-DFc electron density maps with contour level 1σ and extent radius 5 \AA are centered on inhibitor structures and are shown in blue chicken wire for BlaC D179N structures or black chicken wire for BlaC wild-type with vaborbactam. The figures are generated using CCP4mg [45].

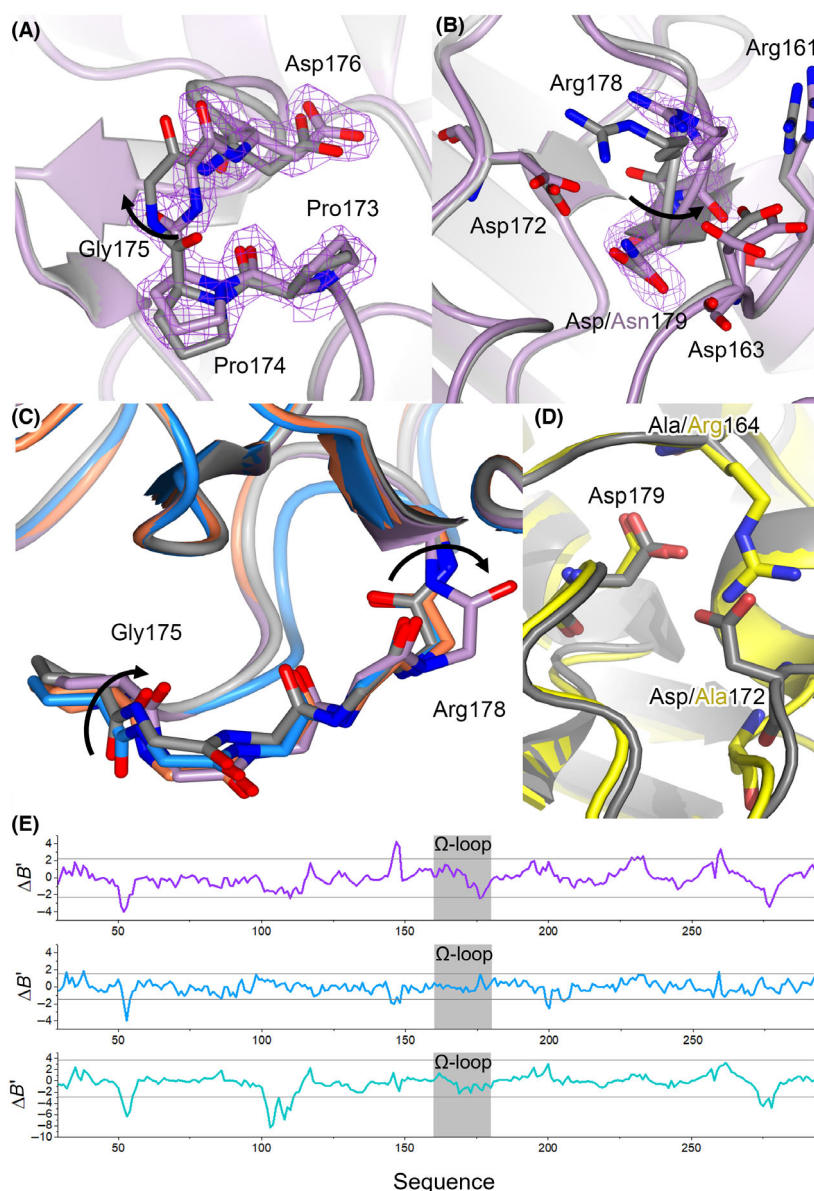
soluble cell fraction. Similarly, for KPC-2 and NMC-A the SDS-PAGE analysis shows the presence of more wild-type than mutant protein in the soluble cell fraction (Fig. 9A), indicating that mutation D179N influences the levels of soluble enzyme.

Discussion

The most common side chain interactions observed in the Ω -loop of class A β -lactamases are Arg161-Asp163, Glu166-Asn170, and Arg164-Asp179. BlaC does not carry Arg at position 164, thus the salt bridge to Asp179 is missing. The importance of this salt bridge was discussed in multiple studies on various class A β -lactamases. It was shown that mutations in both Arg164 and Asp179 increase resistance against ceftazidime, while decreasing the resistance to other β -lactam antibiotics [8,12,20,21,22,23]. The same effect is observed in our study on BlaC, because almost all mutants of

Asp179 cause increased resistance against ceftazidime in *E. coli* and decreased resistance to other compounds. Increased flexibility of Ω -loop has been suggested as an explanation for the shift in substrate profile. A higher ceftazidime minimal inhibitory concentration was also reported for mutant P167S of CTX-M-14, and it was shown that this mutation causes conformational flexibility in Ω -loop and a large rearrangement of the loop in acyl-enzyme complex [24]. In resting state enzyme the loop was structurally similar to that in the wild-type protein, but with acylated adduct it assumed a different conformation, changing the position of the adduct compared to the adduct in the structure of the wild-type enzyme and so influencing the positions of active site residues. We observed a similar behaviour for the same mutation in BlaC, showing that indeed the conformational freedom introduced by this mutation is the reason for its changed substrate profile [15]. The two-phased product formation curve and low melting temperature

Fig. 6. (A,B) Crystal structure of BlaC D179N (PDB entry 8BTU, lilac) overlaid with wild-type structure (PDB entry 2GDN [3], grey), showing the flipped peptide bonds between residues 174 and 175 (A) and 178 and 179 (B). The side chain of Asp163 in BlaC D179N is present in two conformations. The 2mF₀-DF_c electron density of the flipped peptide bonds are represented in purple chicken wire, with contour level 1 σ and extent radius 5 Å; (C) Crystal structure of BlaC wild-type (grey) overlaid with BlaC D179N free form (lilac), with sulbactam adduct (PDB entry 8BTU, orange) and vaborbactam (PDB entry 8BTW, blue). The backbone of the residues 174–179 is shown in sticks. The black arrows indicate the flipped peptide bonds. (D) Overlay of BlaC wild-type (grey) and TEM-1 (PDB entry 1ZG4 [44], yellow) showing the position of the residues 164, 172 and 179. In BlaC the side chain of Asp172 fills part of the space taken by the side chain of Arg164 in TEM; (E) The difference between the normalized B-factors (B') of BlaC D179N and wild-type BlaC in free form (in purple, wild-type structure 5OYO [27] and mutant structure 8BTU), with the vaborbactam adduct (in blue, wild-type structure 8BV4 and mutant structure 8BTW), and with the sulbactam adduct (in turquoise, wild-type structure 6H2K [18] and mutant structure 8BTU). The cutoff for the significant $\Delta B'$ was set to two standard deviations of the mean. The residues 160–180 in the Ω -loop are highlighted in grey. The figures are generated using CCP4mg [45].



observed for BlaC D179G (Table 2, Fig. 2) resemble the behaviour of BlaC P167S and suggest that also this variant exists in more than one conformation, either in the resting state or during the reaction (branched kinetics). Also, for other β -lactamases, studies indicate that mutation in D179 enhances the flexibility of the Ω -loop. Barnes and colleagues [11] used modelling to predict the changes in the Ω -loop occurring upon mutation of Asp179 in KPC-2, indicating loss of the interaction with Arg164 and increased flexibility of Ω -loop. This mobility led to changes in the position of the catalytic residues Ser70 and Glu166. The crystal structure of KPC-2 D179N showed that the disruption of 179–164 interaction results in a displacement of the active site residue

Asn170 [6]. This change was accompanied by the drastic decrease in the stability of the protein. The studies on the KPC D179Y variant showed that this mutation leads to a disordering of the Ω -loop, which was linked to an improved ceftazidime degradation [6,25]. Increased flexibility of the Ω -loop was also observed in the crystal structure of PC1 D179N from *Staphylococcus aureus*, where the Ω -loop was found to be disordered [26]. In the case of BlaC Asp179 variants, the increased conformational freedom of the part of the Ω -loop can be explained by the change in the interaction between Asp172 and residue at position 179. Crystal structures of D179N BlaC indicated the possibility for the peptide bonds between these two residues to flip, which is likely

Table 4. Sequence identity as determined by ClustalOmega and RMSD as determined with PyMOL when aligning by structure (Uniprot entries P9WKD3–1, Q9L5C7, Q9F663, P52663, P62593, and PDB entries 2GDN [3], 1YLT [41], 2OV5 [42], 1BUE [43], and 1ZG4 [44]).

Sequence identity (%)						
Structural RMSD (Å)	BlaC	CTX-M-14	KPC-2	NMC-A	TEM-1	Average
BlaC		45	48	41	35	42
CTX-M-14	0.728		54	49	38	46
KPC-2	0.771	0.569		58	40	50
NMC-A	0.964	0.861	0.600		35	45
TEM-1	0.702	0.638	0.693	0.927		37
Average	0.791	0.699	0.658	0.838	0.740	

caused by a new hydrogen bond interaction between Asn179 and Asp172, which may be less rigid than the carboxyl-carboxylate interaction in the wild-type enzyme. The absence of this hydrogen bond in BlaC D179G might lead to even more conformational freedom in the Ω -loop. Although NMR data and the normalized B-factor analysis of the crystal structures provide no indication of increased flexibility of the Ω -loop in the D179N variant, the changes in the peptide bonds observed in the crystal structures indicate the ability of this variant to adapt the conformation of the loop to the specific substrate or inhibitor. Such slight enhancement of conformational freedom may enable the enhanced ceftazidime enhancement while maintaining the activity against other substrates.

Here, we tested the effects of D179N in five β -lactamases that are representative for the class A β -lactamases. *E. coli* producing this variant of KPC-2, NMC-A and TEM-1 are more sensitive to penicillins and meropenem and less to ceftazidime, in line with fitness studies on TEM-1 and KPC-2 [8,11]. In CTX-M-14, the D179N substitution impacts the ability of the cells producing this variant to grow in presence of all tested antibiotics, probably because the solubility of the enzyme is compromised by the mutation. These findings, together with the previous findings described in the literature, suggest that in all cases the Ω -loop is more mobile, enhancing activity against ceftazidime or, in the case of CTX-M-14, to such an extent that the protein is no longer stable and becomes insoluble. These observations make BlaC D179N an interesting exception. Mutation to other residues of Asp179 in BlaC also leads to a reduced melting temperature and a shift in the substrate spectrum toward ceftazidime activity. BlaC D179N, however, is produced as a soluble protein with high yield, shows a single conformation in the NMR spectrum, with no evidence of extensive line-broadening, and yields a crystal structure with an ordered Ω -loop. At the same time, it shows somewhat enhanced activity against ceftazidime as well

as good activity against penicillins and nitrocefin. Position 164 is occupied predominantly by Arg in class A β -lactamases, while BlaC carries Ala at this position. The H-bond between Asp172 and Asp179 in BlaC is only possible due to the absence of Arg at position 164, because the side chains of Arg164 and Asp172 would clash (Fig. 6D). This subtle change could be responsible for differences observed upon mutation in Asp179 in BlaC vs. other β -lactamases. The D179N in BlaC appears to strike a balance that enhances stability and yet slightly increases Ω -loop flexibility. In other β -lactamases the mutation introduces flexibility and reduced stability due to the lost salt bridge between Asp179 and Arg164. Asp179 is highly conserved in class A β -lactamases, and so is Arg164, thus it is possible that being able to cope with the loss of this Arg, opens a new evolutionary pathway to BlaC by introducing the D179N mutation to stabilize the enzyme and at the same time enhance its substrate spectrum.

Materials and methods

β -Lactamase activity in bacterial cells

Resistance assays were performed with *E. coli* KA797 cells transformed with pUK21 based plasmids with a TAT-signal sequence [19] and containing the *blaC*, *blaCTX-M-14*, *kpc*, *nmcA* or *bla* wild-type or mutant genes, coding for the soluble parts of BlaC, CTX-M-14, KPC-2, NMC-A and TEM-1, respectively (Fig. 7). For the on-plate assay, cells were applied on the agar plates with various β -lactam antibiotics as 10 μ L drops with OD₆₀₀ values of 0.3, 0.03, 0.003 and 0.0003. All plates contained 50 μ g mL⁻¹ kanamycin and 1 mM IPTG and were incubated for 16 h at 37 °C. In pUK21 the *bla* genes are under the control of the *lac* promoter but the used strain did not overproduce the LacI inhibitor, so production of the β -lactamases was semi-constitutive due to the high copy number of the plasmid. IPTG was added to ensure complete release of inhibition. For the assay with bacterial suspensions, cells with the

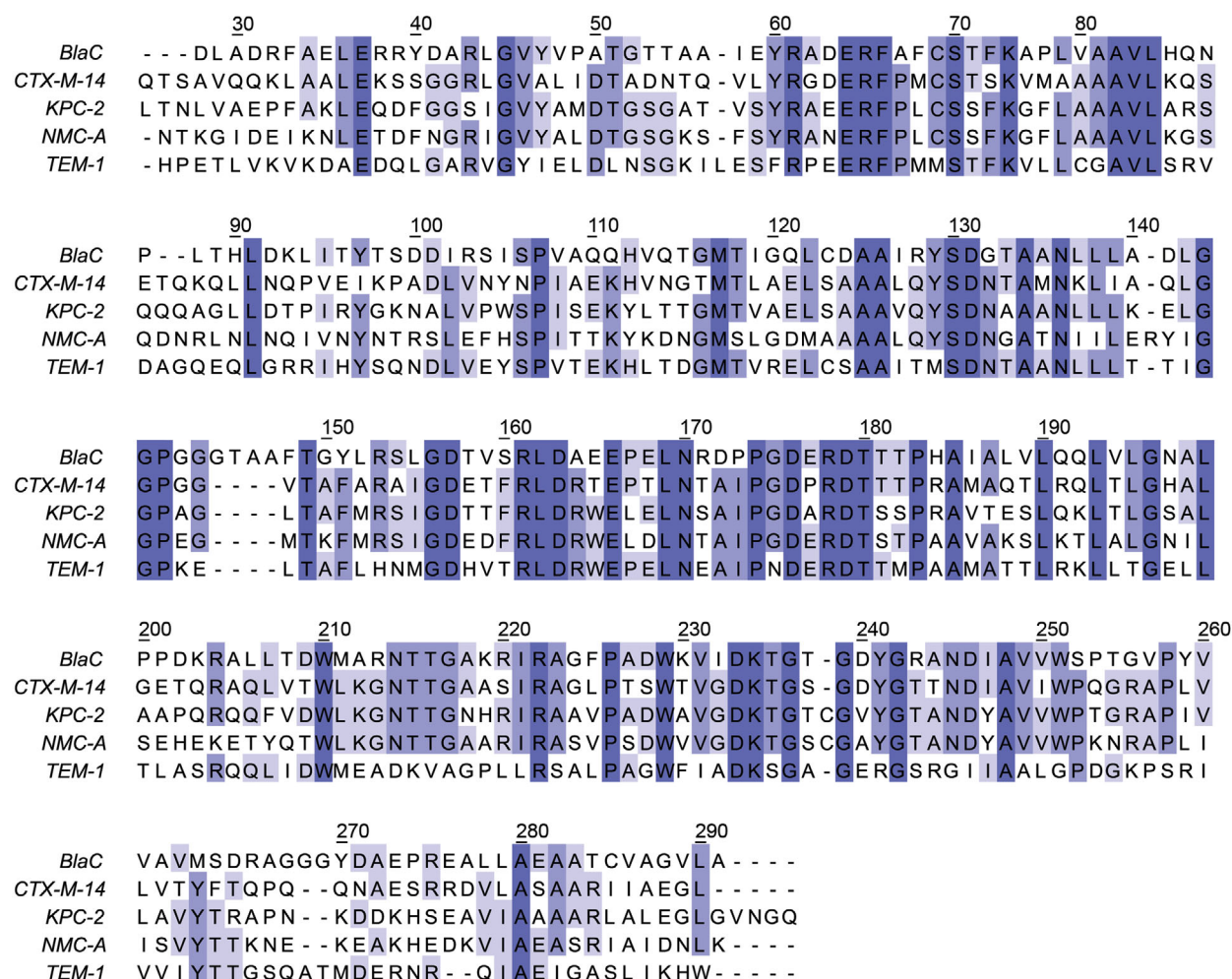


Fig. 7. Sequences of β -lactamases. Residues are numbered according to Ambler notation, and correspond to residue numbers 43–307 of BlaC Uniprot entry P9WKD3-1, 29–291 of CTX-M-14 Uniprot entry Q9L5C7, 25–293 of KPC-2 Uniprot entry Q9F663, 28–292 of NMC-A Uniprot entry P52663, and 24–286 of TEM-1 Uniprot entry P62593. The purple shading indicates the degree of sequence identity. For in cell studies, these sequences are preceded by a TAT-signal sequence, for *in vitro* studies a N-terminal TEV cleavable HIS-tag was added [19]. The alignment is generated using Clustal Omega [40] and visualized using Jalview [46].

OD₆₀₀ 0.3 were diluted 100-fold in LB medium and incubated overnight at 37 °C with constant shaking. Measurements were performed with Bioscreen C plate reader.

Protein production and purification

β -Lactamases were produced using *E. coli* BL21 (DE3) pLysS cells transformed with pET28a plasmids containing the T7 promoter. The same genes as used for the bacterial cell assays (Fig. 7) but without the signal sequences and with an N-terminal His-tag and TEV cleavage site were used for this cytoplasmic overexpression system [19]. BlaC was produced and purified as described previously [27]. For experiments comparing wild-type and D179N variants of various β -lactamases, the pellets from 10 mL overnight

cultures were lysed in 200 μ L of BPER (Thermo Scientific, Rockford, IL, USA) for 30 min. After centrifugation, the soluble fraction was diluted 50-fold in 100 mM sodium phosphate buffer pH 6.4 and used for circular dichroism spectroscopy and kinetic experiments. Protein solubility was determined by running samples of the whole lysate and the soluble fraction on a 4–15% Mini-PROTEAN TGX Stain-Free Protein Gel (BioRad, Hercules, CA, USA).

Circular dichroism spectroscopy

Circular dichroism spectra were recorded in a 1 mm quartz cuvette at 25 °C with a Jasco J-815 spectropolarimeter. Samples contained 100 mM sodium phosphate buffer (pH 6.4). The curves represent the average of five transients.

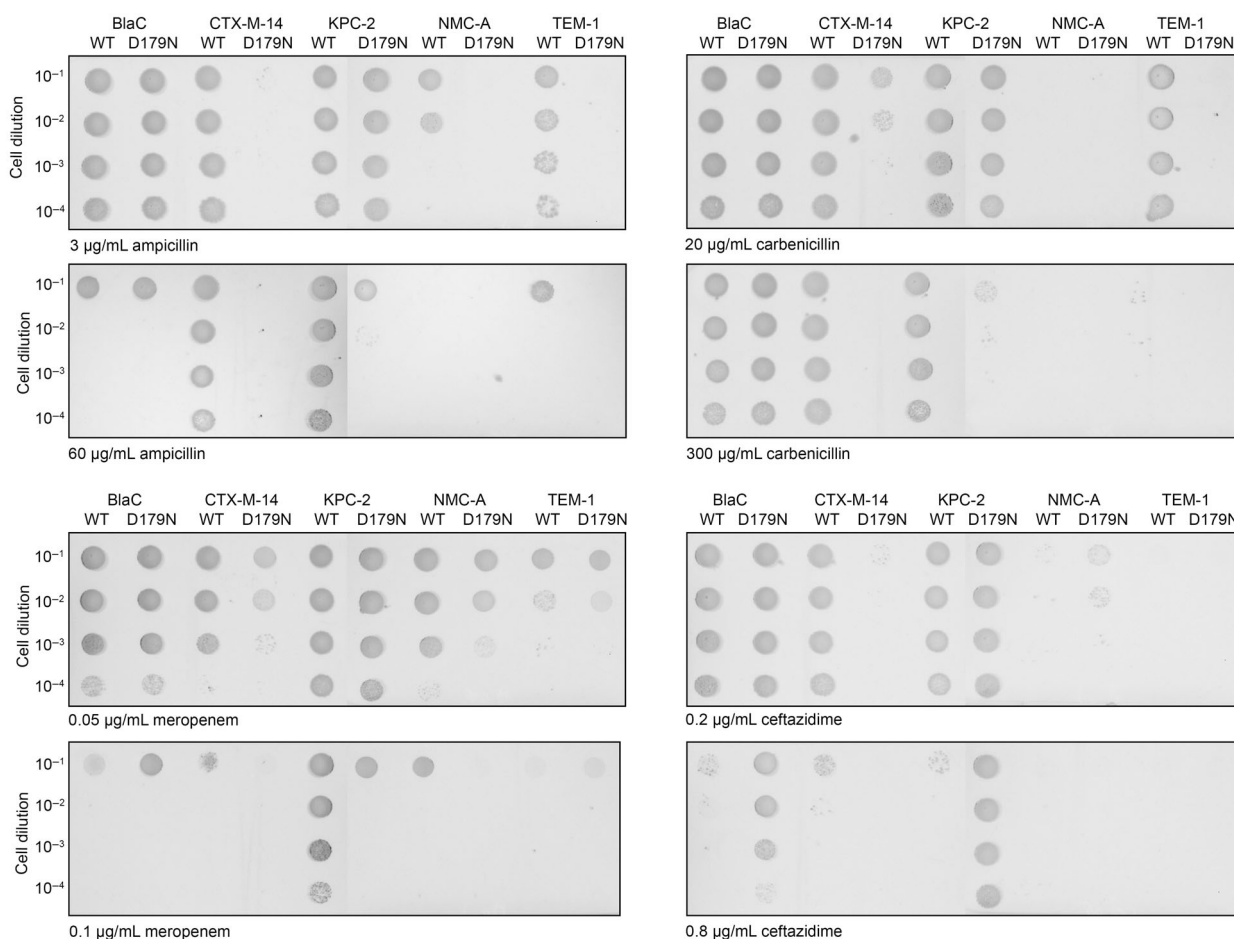


Fig. 8. Activity against antibiotics of five class A beta-lactamases. Cultures of *E. coli* expressing genes of the wild-type or D179N variants of β -lactamases BlaC, CTX-M-14, KPC-2, NMC-A or TEM-1 were spotted in increasing dilution on plates containing ampicillin, carbenicillin, meropenem or ceftazidime. Different panels within black border originate from different parts of the same LB-agar plates (Figs S4–S7).

Melting temperature

Thermostability of BlaC variants was determined with the use of the hydrophobic dye SYPRO[®] Orange (Sigma-Aldrich, St. Louis, MO, USA) or using tryptophan fluorescence changes. The commercially available stock of SYPRO[®] Orange dye has a 5000 \times concentration, but a 4 \times concentration was used in the measurements. Tryptophan fluorescence was measured as a function of temperature using a Tycho NT.6 (NanoTemper Technologies, München, Germany) at 330 nm and 350 nm and the ratio 330 nm/350 nm was used to evaluate the melting temperature. All measurements were done in triplicate in 100 mM sodium phosphate buffer (pH 6.4).

Kinetics

Kinetic experiments for BlaC D179 variants were performed using a Lambda 800 UV-vis spectrometer (PerkinElmer,

Waltham, MA, USA) at 25 °C in 100 mM sodium phosphate buffer (pH 6.4). For nitrocefin kinetics 5 nM of enzyme was used with 0, 10, 25, 50, 100, 200, 300, and 400 μ M of nitrocefin ($\Delta\epsilon_{486} = 18 \times 10^3 \text{ cm}^{-1} \text{ M}^{-1}$). The reactions were followed at 486 nm for 90 s in triplicate. The initial velocities were fitted to the Michaelis–Menten, Eqn (1). v_0 is the initial reaction rate, $[S]_0$ the initial substrate concentration, V_{max} the maximum reaction rate and K_M the Michaelis constant. v_0 and $[S]_0$ are the dependent and independent variables, respectively, and K_M and V_{max} are the fitted parameters. V_{max} is equal to the product of the specific rate constant (k_{cat}) and the enzyme concentration. Note that due to the two-step reaction of antibiotic hydrolysis, the K_M must be considered as apparent value that cannot be directly compared with the K_M from the Michaelis–Menten derivation.

$$v_0 = \frac{V_{\text{max}} [S]_0}{K_M + [S]_0} \quad (1)$$

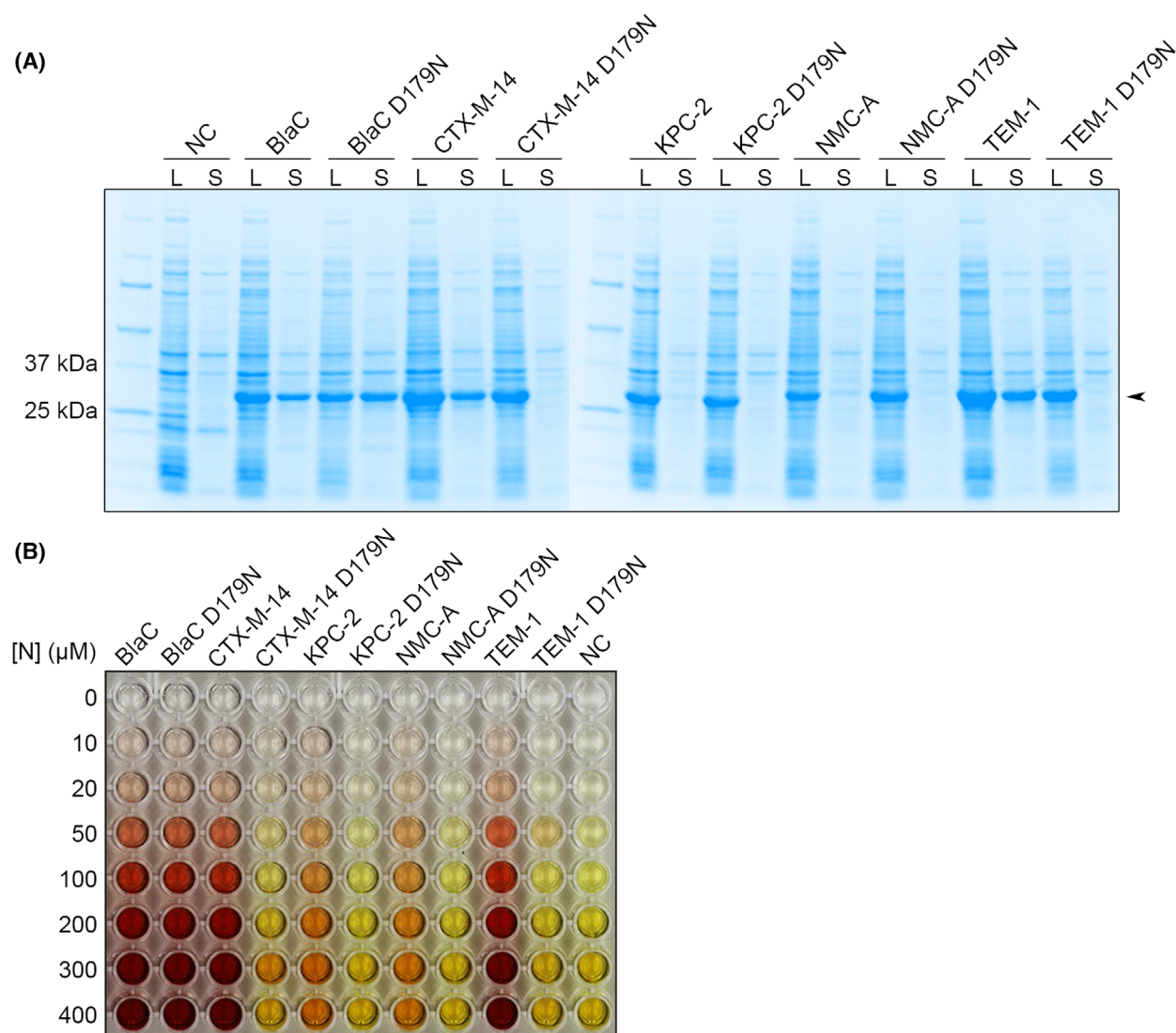


Fig. 9. Effects of D179N mutation on several β -lactamases. (A) SDS-PAGE analysis shows the whole lysate (L) and soluble fractions (S) of negative control (NC), BlaC (31.5 kDa), CTX-M-14 (31.3 kDa), KPC-2 (31.8 kDa), NMC-A (32.4 kDa), and TEM-1 (32.2 kDa), indicated by an arrow. Samples were corrected for cell density; (B) Activity in nitrocefin conversion using soluble cell fractions of cultures overproducing the indicated β -lactamases was measured in 96-well plates containing the indicated nitrocefin (N) concentration. Upon ring opening, nitrocefin turns from yellow to red. The picture was taken 30 min after the start of the reactions.

To measure the hydrolysis of ceftazidime for Fig. 3D, 1 μM of BlaC was mixed with 20 μM ceftazidime. Substrate degradation was followed at 260 nm for 7 min in duplicate, using an extinction coefficient difference ($\Delta\epsilon_{260}$) of 6.8 ± 0.9 ($\times 10^3$) $\text{M}^{-1}\cdot\text{cm}^{-1}$ [15]. The kinetic parameters of the ceftazidime hydrolysis reaction were determined with 100 nM of BlaC and 10, 25, 50 and 100 μM of ceftazidime. The reactions were followed at 260 nm for 5 min and performed in duplicate. In case of biphasic behaviour (Fig. 3E) of the reaction, the velocities of the second phase (steady state condition) were calculated and plotted against substrate concentration. For wild-type BlaC and BlaC

D179N the determination of the K_M and V_{max} values was not possible because $K_M \gg [S]$, so k_{cat}/K_M values were determined from $v_0/[S]$. Activity in lysates was determined by mixing the 50 \times diluted soluble fraction of cell lysates with 0, 10, 20, 50, 100, 200, 300 and 400 μM of nitrocefin at 25 $^\circ\text{C}$.

Inhibition assay

To measure the BlaC inhibition by avibactam, 2.5 nM of BlaC was used with 100 μM nitrocefin in the presence of increasing amounts of avibactam, 0, 10, 100 and 500 μM .

The reactions were followed at 486 nm for 20 min and the experiments were performed in duplicate.

NMR spectroscopy experiments

^{13}C , ^{15}N enriched (98%) protein was produced as described previously [27]. TROSY-HSQC [28,29] and HNCA spectra were recorded on a AVIII HD 850 MHz spectrometer (Bruker Biospin, Leiden, The Netherlands) at 25 °C on a sample of 1 mM BlaC in 100 mM phosphate buffer (pH 6.4) with 6% D_2O in a 5 mm NMR tube. Data were processed in Topspin 4.0.7 (Bruker Biospin). Spectra were analysed with CCPNmr Analysis software V3 [30]. Amide resonances were assigned for BlaC D179N by comparison to peaks in the wild-type BlaC spectrum [27,31] and confirmed using the HNCA spectrum. Average chemical shift perturbations (CSP), $\Delta\delta$, of the ^1H ($\Delta\omega_1$) and ^{15}N ($\Delta\omega_2$) resonances of backbone amides were calculated using Eqn (2).

$$\Delta\delta = \sqrt{\frac{1}{2} \left(\Delta\omega_1^2 + \left(\frac{\Delta\omega_2}{5} \right)^2 \right)} \quad (2)$$

Crystallization

Crystallization conditions for BlaC D179N at a concentration of 10 mg mL⁻¹ were screened for by the sitting-drop method using the JCSG+, BCS and Morpheus (Molecular Dimensions, Catcliffe, UK) screens at 20 °C with 200 nL drops with 1:1 protein to screening condition ratio [32]. Crystal growth became visible within 4 days in various conditions specified in Table S1. After 1 month the crystals were mounted on cryoloops in mother liquor and vitrified by plunging in liquid nitrogen. The crystals of BlaC bound to the inhibitors were soaked in corresponding mother liquor with 10 mM sulbactam or vaborbactam for 20–40 min.

X-ray data collection, processing and structure solving

Diffraction data were collected at the Diamond Light Source (DLS, Oxford, England). Diffraction data were recorded on a Pilatus detector. The resolution cutoff was determined based on completeness and CC1/2 values. The data were integrated using DIALS [33] and scaled using Aimless [34]. The structures were solved by molecular replacement using MOLREP from the CCP4 suite [35] using PDB entry 2GDN [3] as a search model for all structures except for BlaC D179N with sulbactam for which 6H2K [18] was used as a search model. Subsequently, building and refinement were performed using Coot and REFMAC [35]. Waters were added in REFMAC during refinement. The following residues were modelled in two

conformations: Asp163 for BlaC D179N; Lys230 for BlaC D179N with sulbactam; and Asn197 for BlaC D179N with vaborbactam. The final models fall on the 98th–99th percentile of MolProbity [36]. The models were further optimized using the PDB-REDO webserver [37,38]. Structure validation showed a RamaZ score [38] of -0.15, -0.27, -0.44, and -1.82 for D179N, D179N with sulbactam, D179N with vaborbactam, and wild-type BlaC with vaborbactam respectively; 97%–99% of all residues are within the Ramachandran plot favoured regions with two outliers for all structures, namely, Cys69 and Arg220. Data collection and refinement statistics can be found in Table S1. The normalized B-factor analysis was performed using BANAIT server [39]. The Gly145A/B/C/D insertion in one of the loops of BlaC was excluded from the analysis for all structures as it differs considerably even between the wild-type BlaC structures available.

Structural and sequential analysis

Sequence identity was calculated by Clustal Omega [40] using 497 sequences of class A β -lactamases without signal sequence. 494 originate from the broad mutagenesis study [1], which include BlaC and CTX-M-14. The sequences of BlaC, CTX-M-14, KPC-2, NMC-A and TEM-1 correspond to Uniprot entries P9WKD3, Q9L5C7, Q9F663, P52663 and P62593, respectively. Structural analysis was done using the PDB structures 2GDN [3], 1YLT [41], 2OV5 (subunit A) [42], 1BUE [43], and 1ZG4 [44] for BlaC, CTX-M-14, KPC-2, NMC-A, and TEM-1, respectively. Root mean square deviations (RMSD) were calculated by a sequence-independent structure-based alignment in The PyMOL Molecular Graphics System, Version 2.5.0 (Schrödinger, LLC, New York, NY, USA).

Author contributions

IvA, AC, and MU designed the experiments. IvA, AC, DBvZ, AAdB, and MT executed the experiments. IvA, AC, SB, and MU analysed the data. IvA, AC, and MU wrote the article.

Acknowledgements

We thank Patrick Voskamp for technical support, Robbert Q. Kim for collection of the crystallography data and Jing Sun for providing the extinction coefficient for ceftazidime hydrolysis. We acknowledge the Diamond Light Source (DLS), Oxford, England for provision of synchrotron radiation facilities. We acknowledge the Dutch Research Council for funding (711.016.002 and 711.017.013 to MU). We declare no competing financial interest.

Conflict of interest

The authors declare no conflict of interest.

Peer review

The peer review history for this article is available at <https://www.webofscience.com/api/gateway/wos/peer-review/10.1111/febs.16892>.

Data availability statement

NMR chemical shift assignments have been submitted to the Biological Magnetic Resonance Data Bank (BMRB) and can be accessed under BMRB accession number 51702. The crystal structures and data files of free form BlaC D179N, and BlaC D179N bound to sulbactam or vaborbactam and wild-type BlaC bound to vaborbactam have been submitted to the Protein Data Bank (PDB) and can be accessed under accession numbers [8BTU](#), [8BTV](#), [8BTW](#), and [8BV4](#), respectively.

References

- Chikunova A & Ubbink M (2022) The roles of highly conserved, non-catalytic residues in class A β -lactamases. *Protein Sci* **31**, e4328.
- Ambler RP, Coulson AFW, Frère JM, Ghuysen JM, Joris B, Forsman M, Levesque RC, Tiraby G & Waley SG (1991) A standard numbering scheme for the class a β -lactamases. *Biochem J* **276**, 269–270.
- Wang F, Cassidy C & Sacchettini JC (2006) Crystal structure and activity studies of the *Mycobacterium tuberculosis* β -lactamase reveal its critical role in resistance to β -lactam antibiotics. *Antimicrob Agents Chemother* **50**, 2762–2771.
- Ibuka AS, Ishii Y, Galleni M, Ishiguro M, Yamaguchi K, Frère JM, Matsuzawa H & Sakai H (2003) Crystal structure of extended-spectrum β -lactamase Toho-1: insights into the molecular mechanism for catalytic reaction and substrate specificity expansion. *Biochemistry* **42**, 10634–10643.
- Minasov G, Wang X & Shoichet BK (2002) An ultrahigh resolution structure of TEM-1 β -lactamase suggests a role for Glu166 as the general base in acylation. *J Am Chem Soc* **124**, 5333–5340.
- Alsenani TA, Viviani SL, Kumar V, Taracila MA, Bethel CR, Barnes MD, Papp-Wallace KM, Shields RK, Nguyen MH, Clancy CJ *et al.* (2022) Structural characterization of the D179N and D179Y variants of KPC-2 β -lactamase: Ω -loop destabilization as a mechanism of resistance to ceftazidime-avibactam. *Antimicrob Agents Chemother* **66**, e02414–e02421.
- Vakulenko SB, Tóth M, Taibi P, Mobashery S & Lerner SA (1995) Effects of Asp-179 mutations in TEM_{pUC19} β -lactamase on susceptibility to β -lactams. *Antimicrob Agents Chemother* **39**, 1878–1880.
- Vakulenko SB, Taibi-Tronche P, Tóth M, Massova I, Lerner SA & Mobashery S (1999) Effects on substrate profile by mutational substitutions at positions 164 and 179 of the class a TEM_{pUC19} β -lactamase from *Escherichia coli*. *J Biol Chem* **274**, 23052–23060.
- Gonzalez CE, Roberts P & Ostermeier M (2019) Fitness effects of single amino acid insertions and deletions in TEM-1 β -lactamase. *J Mol Biol* **431**, 2320–2330.
- Firnberg E, Labonte JW, Gray JJ & Ostermeier M (2014) A comprehensive, high-resolution map of a gene's fitness landscape. *Mol Biol Evol* **31**, 1581–1592.
- Barnes MD, Winkler ML, Taracila MA, Page MG, Desarbre E, Kreiswirth BN, Shields RK, Nguyen M-H, Clancy C, Spellberg B *et al.* (2017) *Klebsiella pneumoniae* Carbapenemase-2 (KPC-2), substitutions at Ambler position Asp179, and resistance to ceftazidime-avibactam: unique antibiotic-resistant phenotypes emerge from β -lactamase protein engineering. *MBio* **8**, e00528-17.
- Levitt PS, Papp-Wallace KM, Taracila MA, Hujer AM, Winkler ML, Smith KM, Xu Y, Harris ME & Bonomo RA (2012) Exploring the role of a conserved class A residue in the Ω -loop of KPC-2 β -lactamase: a mechanism for ceftazidime hydrolysis. *J Biol Chem* **287**, 31783–31793.
- Stojanoski V, Chow DC, Hu L, Sankaran B, Gilbert HF, Prasad BVV & Palzkill T (2015) A triple mutant in the Ω -loop of TEM-1 β -lactamase changes the substrate profile via a large conformational change and an altered general base for catalysis. *J Biol Chem* **290**, 10382–10394.
- Papp-Wallace KM, Becka SA, Taracila MA, Winkler ML, Gatta JA, Rholl DA, Schweizer HP & Bonomo RA (2016) Exposing a β -lactamase “twist”: the mechanistic basis for the high level of ceftazidime resistance in the C69F variant of the *Burkholderia pseudomallei* PenI β -lactamase. *Antimicrob Agents Chemother* **60**, 777–788.
- Sun J, Chikunova A, Boyle AL, Voskamp P, Timmer M, Ubbink M (2023) Enhanced activity against a third-generation cephalosporin by destabilization of the active site of a class A beta-lactamase. Under revision.
- Sawyer L & James MNG (1982) Carboxyl–carboxylate interactions in proteins. *Nature* **295**, 79–80.
- Lin J, Pozharski E & Wilson MA (2017) Short carboxylic acid-carboxylate hydrogen bonds can have fully localized protons. *Biochemistry* **56**, 391–402.
- Tassoni R, Blok A, Pannu NS & Ubbink M (2019) New conformations of acylation adducts of inhibitors of β -lactamase from *Mycobacterium tuberculosis*. *Biochemistry* **58**, 997–1009.

- 19 van Alen I, Chikunova A, Safeer AA, Ahmad MUD, Perrakis A & Ubbink M (2021) The G132S mutation enhances the resistance of *Mycobacterium tuberculosis* β -lactamase against sulbactam. *Biochemistry* **60**, 2236–2245.
- 20 Castanheira M, Arends SJR, Davis AP, Woosley LN, Bhalodi AA & MacVane SH (2018) Analyses of a ceftazidime-avibactam-resistant *Citrobacter freundii* isolate carrying *bla_{KPC-2}* reveals a heterogenous population and reversible genotype. *mSphere* **3**, e00408-18.
- 21 Bonomo R (1997) OHIO-1 β -lactamase mutants: Asp179Gly mutation confers resistance to ceftazidime. *FEMS Microbiol Lett* **152**, 275–278.
- 22 Winkler ML, Papp-Wallace KM & Bonomo RA (2015) Activity of ceftazidime/avibactam against isogenic strains of *Escherichia coli* containing KPC and SHV β -lactamases with single amino acid substitutions in the Ω -loop. *J Antimicrob Chemother* **70**, 2279–2286.
- 23 Majiduddin FK & Palzkill T (2003) An analysis of why highly similar enzymes evolve differently. *Genetics* **163**, 457–466.
- 24 Patel MP, Hu L, Stojanoski V, Sankaran B, Prasad BVV & Palzkill T (2017) The drug-resistant variant P167S expands the substrate profile of CTX-M β -lactamases for oxyimino-cephalosporin antibiotics by enlarging the active site upon acylation. *Biochemistry* **56**, 3443–3453.
- 25 Taracila MA, Bethel CR, Hujer AM, Papp-Wallace KM, Barnes MD, Rutter JD, VanPelt J, Shurina BA, van den Akker F, Clancy CJ *et al.* (2022) Different conformations revealed by NMR underlie resistance to ceftazidime/avibactam and susceptibility to meropenem and imipenem among D179Y variants of KPC β -lactamase. *Antimicrob Agents Chemother* **66**, e02124-21.
- 26 Herzberg O, Kapadia G, Blanco B, Smith TS & Coulson A (1991) Structural basis for the inactivation of the P54 mutant of β -lactamase from *Staphylococcus aureus* PC1. *Biochemistry* **30**, 9503–9509.
- 27 Elings W, Tassoni R, Van Der Schoot SA, Luu W, Kynast JP, Dai L, Blok AJ, Timmer M, Florea BI, Pannu NS *et al.* (2017) Phosphate promotes the recovery of *Mycobacterium tuberculosis* β -lactamase from clavulanic acid inhibition. *Biochemistry* **56**, 6257–6267.
- 28 Pervushin K, Riek R, Wider G & Wüthrich K (1997) Attenuated T2 relaxation by mutual cancellation of dipole–dipole coupling and chemical shift anisotropy. *Proc Natl Acad Sci USA* **94**, 12366–12371.
- 29 Schanda P, Van Melckebeke H & Brutscher B (2006) Speeding up three-dimensional protein NMR experiments to a few minutes. *J Am Chem Soc* **128**, 9042–9043.
- 30 Vranken WF, Boucher W, Stevens TJ, Fogh RH, Pajon A, Llinas M, Ulrich EL, Markley JL, Ionides J & Laue ED (2005) The CCPN data model for NMR spectroscopy: development of a software pipeline. *Proteins* **59**, 687–696.
- 31 Chikunova A, Manley MP, Ud Din Ahmad M, Bilman T, Perrakis A & Ubbink M (2021) Conserved residues Glu37 and Trp229 play an essential role in protein folding of β -lactamase. *FEBS J* **288**, 5708–5722.
- 32 Newman J, Egan D, Walter TS, Meged R, Berry I, Ben Jelloul M, Sussman JL, Stuart DI & Perrakis A (2005) Towards rationalization of crystallization screening for small- to medium-sized academic laboratories: the PACT/JCSG+ strategy. *Acta Crystallogr D Biol Crystallogr* **61**, 1426–1431.
- 33 Clabbers MTB, Gruene T, Parkhurst JM, Abrahams JP & Waterman DG (2018) Electron diffraction data processing with DIALS. *Acta Crystallogr D Struct Biol* **74**, 506–518.
- 34 Evans PR (2011) An introduction to data reduction: space-group determination, scaling and intensity statistics. *Acta Crystallogr D Biol Crystallogr* **67**, 282–292.
- 35 Winn MD, Ballard CC, Cowtan KD, Dodson EJ, Emsley P, Evans PR, Keegan RM, Krissinel EB, Leslie AGW, McCoy A *et al.* (2011) Overview of the CCP4 suite and current developments. *Acta Crystallogr D Biol Crystallogr* **67**, 235–242.
- 36 Chen VB, Arendall WB III, Headd JJ, Keedy DA, Immormino RM, Kapral GJ, Murray LW, Richardson JS & Richardson DC (2010) MolProbity: all-atom structure validation for macromolecular crystallography. *Acta Crystallogr D Biol Crystallogr* **66**, 12–21.
- 37 Joosten RP, Long F, Murshudov GN & Perrakis A (2014) The PDB-REDO server for macromolecular structure model optimization. *IUCrJ* **1**, 213–220.
- 38 Sobolev OV, Afonine PV, Moriarty NW, Hekkelman ML, Joosten RP, Perrakis A & Adams PD (2020) A global Ramachandran score identifies protein structures with unlikely stereochemistry. *Structure* **28**, 1249–1258.
- 39 Barthels F, Schirmeister T & Kersten C (2021) BAN Δ IT: B'-factor analysis for drug design and structural biology. *Mol Inform* **40**, 2000144.
- 40 Sievers F, Wilm A, Dineen D, Gibson TJ, Karplus K, Li W, Lopez R, McWilliam H, Remmert M, Söding J *et al.* (2011) Fast, scalable generation of high-quality protein multiple sequence alignments using Clustal omega. *Mol Syst Biol* **7**, 539.
- 41 Chen Y, Delmas J, Sirot J, Shoichet B & Bonnet R (2005) Atomic resolution structures of CTX-M β -lactamases: extended spectrum activities from increased mobility and decreased stability. *J Mol Biol* **348**, 349–362.
- 42 Ke W, Bethel CR, Thomson JM, Bonomo RA & Van Den Akker F (2007) Crystal structure of KPC-2:

- insights into carbapenemase activity in class A β -lactamases. *Biochemistry* **46**, 5732–5740.
- 43 Swarén P, Maveyraud L, Raquet X, Cabantous S, Duez C, Pédelacq J-D, Mariotte-Boyer S, Mourey L, Labia R, Nicolas-Chanoine M-H *et al.* (1998) X-ray analysis of the NMC-A β -lactamase at 1.64-Å resolution, a class A carbapenemase with broad substrate specificity. *J Biol Chem* **273**, 26714–26721.
- 44 Stec B, Holtz KM, Wojciechowski CL & Kantrowitz ER (2005) Structure of the wild-type TEM-1 β -lactamase at 1.55 Å and the mutant enzyme Ser70Ala at 2.1 Å suggest the mode of noncovalent catalysis for the mutant enzyme. *Acta Crystallogr D Biol Crystallogr* **61**, 1072–1079.
- 45 McNicholas S, Potterton E, Wilson KS & Noble MEM (2011) Presenting your structures: the CCP4mg molecular-graphics software. *Acta Crystallogr D Biol Crystallogr* **67**, 386–394.
- 46 Waterhouse AM, Procter JB, Martin DMA, Clamp M & Barton GJ (2009) Jalview version 2-a multiple sequence alignment editor and analysis workbench. *Bioinformatics* **25**, 1189–1191.

Supporting information

Additional supporting information may be found online in the Supporting Information section at the end of the article.

Table S1. Data collection and refinement statistics for BlaC D179N structures and BlaC WT with vaborbactam.

Fig. S1. Activity against penicillin G and ceftazidime of BlaC Asp179 variants.

Fig. S2. Activity against ampicillin and carbenicillin of BlaC Asp179 variants.

Fig. S3. Overlay of ^1H - ^{15}N TROSY-HSQC spectra for BlaC wild-type and BlaC D179N.

Fig. S4. Activity against ampicillin of five class A beta-lactamases on plate.

Fig. S5. Activity against carbenicillin of five class A beta-lactamases on plate.

Fig. S6. Activity against meropenem of five class A beta-lactamases on plate.

Fig. S7. Activity against ceftazidime of five class A beta-lactamases on plate.

Fig. S8. Activity against ampicillin of five class A beta-lactamases in liquid cultures.

Fig. S9. Activity against carbenicillin of five class A beta-lactamases in liquid cultures.

Fig. S10. Activity against meropenem of five class A beta-lactamases in liquid cultures.

Fig. S11. Activity against ceftazidime of five class A beta-lactamases in liquid cultures.